Identification of *Plasmodium falciparum* Spermidine Synthase Active Site Binders through Structure-Based Virtual Screening

Micael Jacobsson,[†,‡] Magnus Gäredal,[‡] Johan Schultz,[†] and Anders Karlén*[,‡]

iNovacia AB, Lindhagensgatan 133, SE-112 51 Stockholm, Sweden, Department of Medicinal Chemistry, Uppsala University, BMC, Box 574, SE-751 23 Uppsala, Sweden

Received December 21, 2007

Seven novel binders, binding in the active site of *Plasmodium falciparum* spermidine synthase, were identified by structure-based virtual screening. The binding of these compounds was experimentally verified by NMR techniques. Spermidine synthase, an enzyme involved in the polyamine pathway, has been suggested as a target for treating malaria. The virtual screening protocol combined 3D pharmacophore filtering, docking, and scoring, focusing on finding compounds predicted to form interactions mimicking those of a previously known binder. The virtual screen resulted in the selection of 28 compounds that were acquired and tested from 2.6 million starting structures. Two of the seven binders were predicted to bind in the amino substrate binding pocket. Both of these showed stronger binding upon addition of methylthioadenosine, one of the two products of the enzyme, and a known binder and inhibitor. The five other compounds were predicted to bind in the part of the active site where the other substrate, decarboxylated *S*-adenosylmethionine, binds. These five compounds all competed for binding with methylthioadenosine.

Introduction

Malaria is a parasitic disease affecting approximately 3.2 billion people in 107 countries, with between 350 and 500 million clinical malaria episodes every year. The main parasites causing this disease are *Plasmodium falciparum* (*Pf*)[a] and *Plasmodium vivax*. *Pf*-induced malaria causes more than one million deaths every year.[1] Hence, there is an urgent need for novel drug targets and novel drugs to treat this disease.

The polyamine pathway has been suggested as a promising target for treating parasitic protozoan infections, including *Pf* infections.[2–9] The naturally occurring polyamines putrescine, spermidine, and spermine are essential for cell growth and differentiation.[10–15] One specific role for spermidine is its involvement in activation of the eukaryotic initiation factor eIF5 through hypusinulation.[16] In *Plasmodium* (see Figure 1), putrescine is synthesized from ornithine by ornithine decarboxylase (ODC). Together with decarboxylated *S*-adenosylmethionine (dcAdoMet), synthesized from *S*-adenosylmethionine (AdoMet) by *S*-adenosylmethionine decarboxylase (AdoMetDC), putrescine is used to synthesize spermidine by spermidine synthase (SpdSyn). SpdSyn also produces methylthioadenosine (MTA).[6] *Pf* SpdSyn has also been shown to be able to synthesize spermine from spermidine.[17]

The irreversible ODC-inhibitor α-difluoromethylornithine[18] is clinically used to treat *T. brucei gambiense* infections (sleeping sickness)[19] and has also been shown to have effect on *Pf*.[3] Several other inhibitors of AdoMetDC and ODC have been shown to inhibit *Pf* growth in vitro.[4,9] More recently, some simple amines were tested for their in vitro inhibition of SpdSyn as well as *Pf* growth in cell cultures. The most potent SpdSyn inhibitor was 4-methylcyclohexylamine (4MCHA),[17] with an enzyme inhibition IC_{50} of 1.4 μM and a growth inhibition IC_{50} of 34 μM. The crystal structure of *Pf* SpdSyn in complex with MTA was recently solved by the Structural Genomics Consortium (PDB ID 2HTE).[20] Subsequently, the apo structure and the complex with dcAdoMet and 4MCHA and the complex with *S*-adenosyl-1,8-diamino-3-thiooctane (AdoDATO)[21] were solved (PDB ID 2I7C)[22] as well as the complex with spermidine (PDB ID 2PWP).

Structure-based virtual screening has been successful in identifying novel binders for a wide range of targets.[23–29] Employing a combination of 3D pharmacophore filtering, docking, and scoring, we have performed a structure-based virtual screen against *Pf* SpdSyn to identify active-site binders that can be used to develop novel chemical series with the ultimate goal of developing drugs to treat malaria through SpdSyn inhibition. Starting from 2.8 million structures representing approximately 3 million commercially available screening compounds, we selected, acquired, and tested 28 compounds for binding to *Pf* SpdSyn by NMR techniques. This resulted in the identification of seven novel compounds binding in the active site of *Pf* SpdSyn.

Results and Discussion

Virtual Screening. The virtual screening procedure employed in this study is similar to previous studies where pharmacophore filtering has been used in conjunction with docking and scoring to increase enrichment.[30–32] The basic outline of the current method is illustrated in Figure 2. First, Phase was used to filter out compounds that were predicted to be able to form specific interaction that were a priori hypothesized to be important for binding to the SpdSyn active site. Two separate pharmacophore hypotheses were used (see Figure 3). One was based on mimicking the interactions of the adenosine moiety of AdoDATO. Here it was hypothesized that the two hydrogen bonds from the protein backbone to the adenine ring were most

* To whom correspondence should be addressed. Phone: +46 18 4714293. Fax: +46 18 4714474. E-mail: anders.karlen@orgfarm.uu.se.

† iNovacia AB.

‡ Department of Medicinal Chemistry, Uppsala University.

[a] Abbreviations: Pf, *Plasmodium falciparum*; ODC, ornithine decarboxylase; AdoMet, *S*-adenosylmethionine; dcAdoMet, decarboxylated *S*-adenosylmethionine; AdoMetDC, *S*-adenosylmethionine decarboxylase; SpdSyn, spermidine synthase; MTA, methylthioadenosine; 4MCHA, 4-methylcyclohexylamine; AdoDATO, *S*-adenosyl-1,8-diamino-3-thiooctane; STD, saturation transfer difference; DMSO, dimethylsulfoxide; HEPES, 4-(2-hydroxyethyl)-1-piperazineethanesulfonic acid; TCEP, tris(2-carboxyethyl)phosphine; Tris, trishydroxymethylaminomethane.

10.1021/jm7016144 CCC: $40.75
Published on Web 04/12/2008

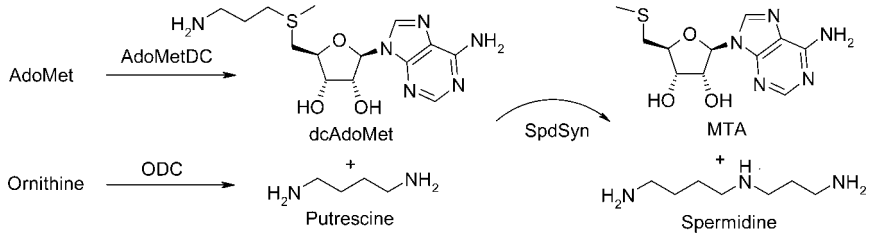

Figure 1. The polyamine pathway of *Pf*.

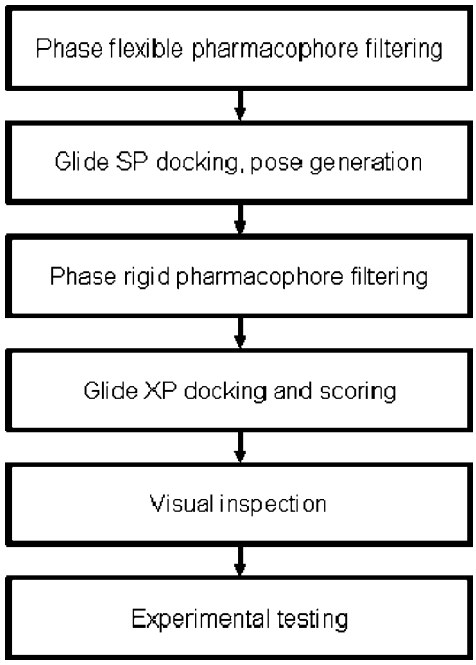

Figure 2. Virtual screening procedure.

important for binding. The flexible pharmacophore search with this pharmacophore yielded 5489 potential binders from 2.6 million candidates. The other pharmacophore hypothesis was based on mimicking the interactions of the diamine substrate. It was hypothesized that the ionic interaction anchoring one of the terminal primary amines to D199, and the narrow hydrophobic "tube" enclosing the butyl part of putrescine as deduced from the AdoDATO complex, were most important for binding. The flexible pharmacophoric search yielded 1866 potential binders. In both cases, the use of excluded volumes to limit the conformational space available to the compounds when trying to match the pharmacophore queries was important to limit the number of hits.

The flexible pharmacophore search in Phase was very fast compared to docking and scoring. For example, the two-point pharmacophore was used to search the 2.6 million compound database with precomputed conformers in five days on four CPUs. Glide SP docking against SpdSyn using the same hardware required approximately 30 s per compound, meaning that docking and scoring 2.6 million compounds using four parallel processes would require more than six months. However, it should be noted that the time required for a specific pharmacophore filtering calculation is highly dependent on the type of pharmacophoric features, the number of features, and the number of required features.

The compounds passing the flexible pharmacophoric search step were expanded to various stereoisomers, tautomers, and protonation states using LigPrep. The resulting structures were docked to the target structure using Glide SP, without any

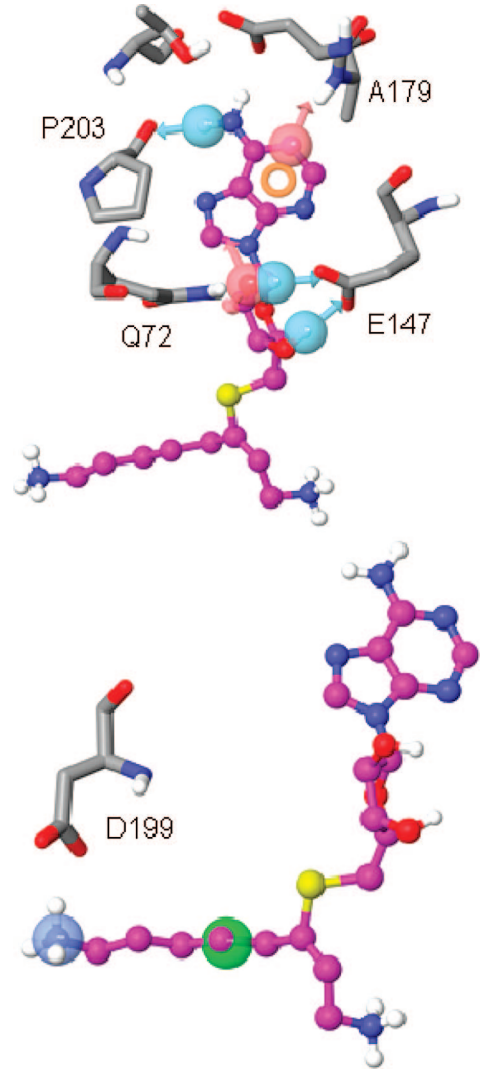

Figure 3. Phase pharmacophore models used in the virtual screen, representing interactions with the adenosine moiety of AdoDATO (top) and amine substrate moiety of AdoDATO (bottom). AdoDATO shown in ball and stick representation with carbons in magenta, selected residues from SpdSyn shown in tube representation. Hydrogen bond donor features shown in light red, acceptor features shown in cyan, aromatic ring features shown in orange, hydrophobic features shown in green, and positively ionizable features shown in blue.

constraints. Nine poses per structure were kept. Subsequently, all poses were matched to the same two pharmacophoric filters but without any conformational flexibility. The version of Phase used in this study, version 2.0, did not allow disabling rigid body translation and rotation of the compounds. Hence, the docked poses were filtered by their ability to match the pharmacophoric filters as freely translated and rotated rigid bodies. In this way, the nine most favorable poses of each compound, as calculated by Glide SP, were automatically filtered

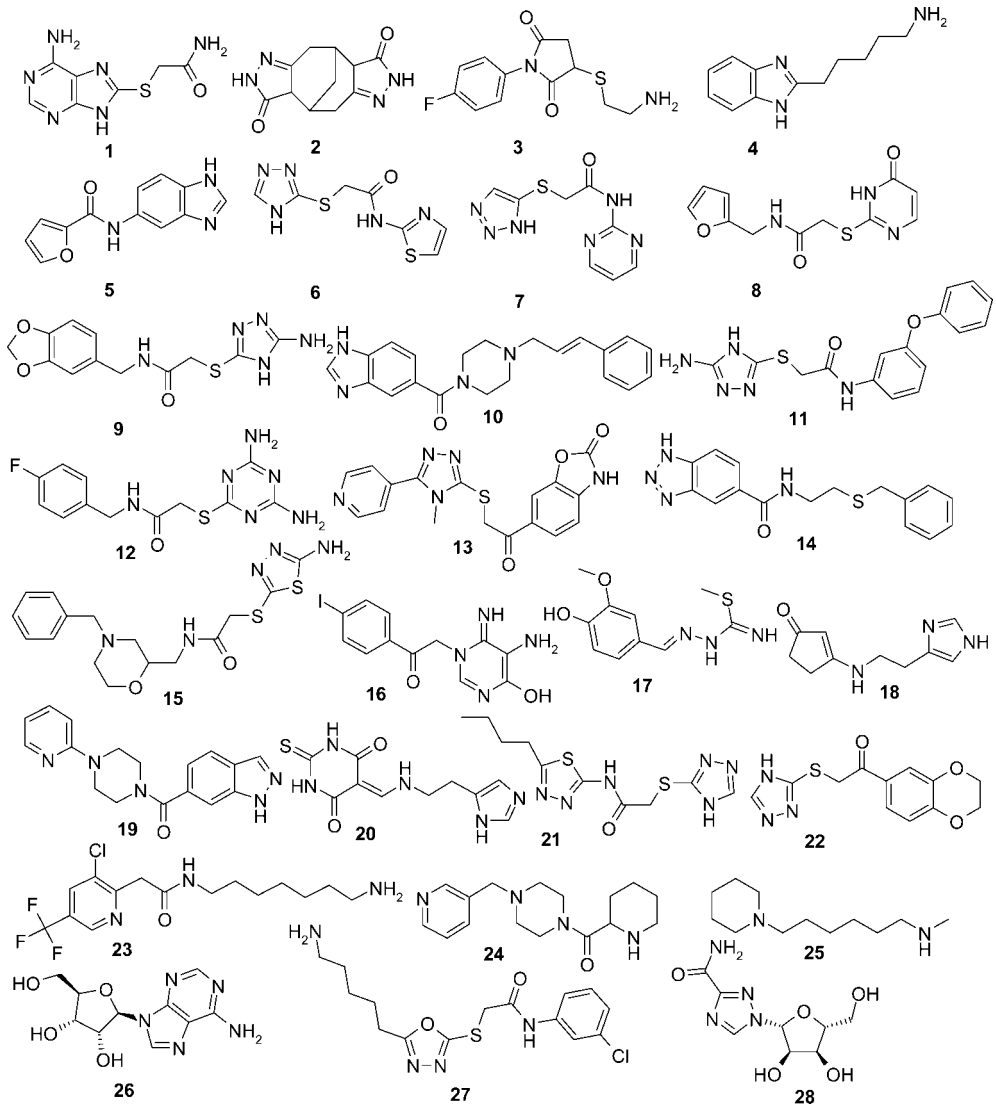

Figure 4. The 28 compounds identified as potential *Pf* SpdSyn active-site binders in the virtual screen.

by their interactions to the target structure. Allowing translational and rotational freedom rendered this step somewhat less discerning than what would otherwise have been the case. The pharmacophore based on the interactions of the adenosine moiety of AdoDATO resulted in 1472 hits from 5489 candidates. The putrescine-pocket pharmacophore yielded 394 hits out of 1866 candidate compounds.

The 1472 plus 394 compounds passing the rigid pharmacophore search filter were again expanded using LigPrep and docked and scored using Glide XP.[33] This is a computationally more expensive docking and scoring algorithm with more elaborate scoring terms and more thorough sampling. At this stage, the automatic pharmacophore filter was not applied. Instead, the highest scoring pose per structure was saved and inspected visually. Then 193 compounds were selected as potential active site binders. These were redocked using Glide XP, storing nine poses per structure. Finally all poses were again inspected visually, and 28 compounds were chosen for acquisition and experimental testing. These are shown in Figure 4. The rank of these compounds in terms of Glide XP score of the best scoring structure for each compound, from the docking and scoring of the 1866 compounds, is shown in Table 1.

The visual inspection of the docked poses focused mainly on the predicted geometry of the hydrogen bonds and deselecting predicted poses with apparently high strain energy, caused by, e.g., internal van der Waals clashes. Compounds with unsuitable functional groups such as thiols or Michael acceptors were also deselected at this stage. This was necessary because no automatic filters for drug-likeness, apart from limiting the molecular weight and number of rotatable bonds, were applied to the compound library prior to the virtual screen.

NMR Binding Experiments. To determine if any of the 28 compounds bind in the active site of *Pf* SpdSyn, they were tested using STD-NMR.[34] In summary, conventional ^{1}H 1D spectra were first collected for compounds in buffer to determine the position of useful proton peaks, i.e., peaks that did not coincide with peaks from DMSO, Tris, glycerol, or MTA. These spectra also revealed whether the compounds were soluble or not and if the ^{1}H 1D spectra agreed with the expected chemical structures. Subsequently, conventional ^{1}H 1D and STD spectra were collected for each compound in the presence of target protein with the compound in molar excess. If a compound binds reversibly to the protein, peaks from the compound will appear in the STD spectrum due to intermolecular saturation transfer, which requires close intermolecular contacts. During the saturation time, the compound molecules must exchange between free and bound state in order to be detected as binders. Thus, only reversible binders will be identified.

Table 1. Ranking in Terms of Docking Score and STD-NMR Binding and Competition Experiment Results for the 28 Compounds Acquired for Experimental Testing

compound	glide XP rank[a]	STD binding	STD competition[b]	compound	glide XP rank	STD binding	STD competition
1	111	binding	competition	**15**	23	no binding	n.a.
2	52	not soluble	n.a.[c]	**16**	98	not soluble	n.a.
3	143	no binding	n.a.	**17**	301	weak binding	maybe competition
4	15	weak binding	stronger binding	**18**	144	no binding	n.a.
5	21	weak binding	maybe competition	**19**	24	no binding	n.a.
6	206	no binding	n.a.	**20**	110	no binding	n.a.
7	59	no binding	n.a.	**21**	1000	no binding	n.a.
8	276	no binding	n.a.	**22**	75	no binding	n.a.
9	83	no binding	n.a.	**23**	41	no binding	n.a.
10	25	binding	partial competition	**24**	44	no binding	n.a.
11	1065	binding	no competition	**25**	169	weak binding	maybe competition
12	1480	no binding	n.a.	**26**	14	binding	competition
13	133	no binding	n.a.	**27**	82	no binding	n.a.
14	162	weak binding	partial competition	**28**	201	no binding	n.a.

[a] Glide XP ranking out of 1866 docked and scored compounds. [b] Competition for binding with 2.5-fold molar excess of MTA over compound. [c] Not applicable.

At this stage, there was no information on the binding site of the compounds. Therefore, another STD binding experiment was performed where each novel binder was mixed with protein and an excess of the known active site binder MTA. If the newly identified binder competes for binding with MTA, the compound peak intensities in the STD spectrum will decrease, and the binding site is most likely the active site. If not, the observed binding takes place somewhere else on the protein, and because there are no other apparent binding pockets in addition to the active site, this binding is likely to be "unspecific" interactions at several low-affinity sites on the protein surface. Because MTA has a relatively low potency (IC_{50} of $159 \pm 27\ \mu M$[17]), complete competition can probably not be expected, at least not when the molar excess of MTA over the other compound is modest. However, partial competition can also mean that the compound binds both in the active site and in other sites.

The results of the STD experiments are shown in Table 1. In summary, there were nine binders, two of which clearly competed for binding with MTA, three which probably competed for binding with MTA, but where the signal-to-noise ratios of the STD signals were too low for unambiguous results, two which were partially competed out by MTA, one which did not compete for binding with MTA, and interestingly, one which clearly showed stronger STD signals when MTA was added. As an example, the NMR STD results for **1** are shown in Figure 5.

To confirm the STD results, a set of $T_{1,\rho}$-relaxation filter NMR experiments[35] were performed for the nine identified binders. The $T_{1,\rho}$-relaxation filter experiment exploits the fact that when a small ligand binds to a macromolecule, the reorientation rate of the small ligand is slowed down. The slower reorientation rate is manifested in a faster transverse relaxation of the ligand protons and a concomitant decrease of signal intensity in the relaxation filtered spectrum. The experiment is performed on two samples that are identical except that the target protein is present in one sample and absent in one, the reference sample. The ligand signal intensities in the two spectra are then compared. If fast exchange and approximately the same on-rate, e.g., diffusion controlled on-rate, is assumed for both compounds, the decrease in signal intensity in the presence of protein can be used to compare the affinities of the two compounds. The higher the affinity, the more pronounced the decrease in signal intensity.[36,37] However, it should be pointed out that in cases where the assumption of fast exchange is not valid, the exchange broadening, and thus the decrease in signal intensity, can be different for two compounds with the same K_D.

In comparison to STD, somewhat higher protein concentrations but lower compound concentrations are required. The lower compound concentration used in the relaxation filter competition experiments allowed a larger molar excess of MTA to be used than that in the STD experiments, approximately 1:63 compared to 1:2.5

The relaxation filter experiment results are shown in Table 2. In summary, the binding was confirmed in all nine cases. Compounds **1** and **26** clearly bound to SpdSyn and competed for binding with MTA, one of which was adenosine. Compounds **10**, **14**, and **17** bound and competed for binding with MTA, but only partially. This most probably means that they bind in the active site of SpdSyn, but that part of the binding signal is due to unspecific binding to the protein. Compound **11** showed no competition with MTA. Consequently, this compound does not bind in the active site of SpdSyn. Compound **5** showed a very small degree of competition with MTA. This compound may be an active site binder, but most of the contribution to the binding signal comes from other binding site(s) not affected by binding of MTA. Finally, compounds **4** and **25**, which were predicted to bind in the amino substrate binding part of the active site, showed stronger binding upon addition of MTA, one much more pronounced than the other. The relaxation filter spectra for **1** and **4** are shown in Figure 6, and all relaxation filter spectra are available as Supporting Information.

Final Results. The virtual screening procedure resulted in 28 compounds being identified as potential binders to *Pf* SpdSyn. Using STD NMR, nine of those were shown to bind reversibly to the target protein. NMR relaxation filter experiments were used to confirm the binders, and seven of the compounds were shown to bind in the active site of *Pf* SpdSyn. On the basis of the decrease of compound signal intensities in the presence of protein compared to the absence of protein, assuming fast exchange and similar on-rates of the compounds, compound **26** (adenosine) and compound **4** (when MTA was added) were the strongest binders, followed by compound **1**. Compounds **25**, **17**, **14**, and **10** were weaker binders. The NMR signals from compound **5** display too low signal-to-noise ratio to unambiguously report this compound as an active site binder. Compound **11** does not bind in the active site and is probably an unspecific binder.

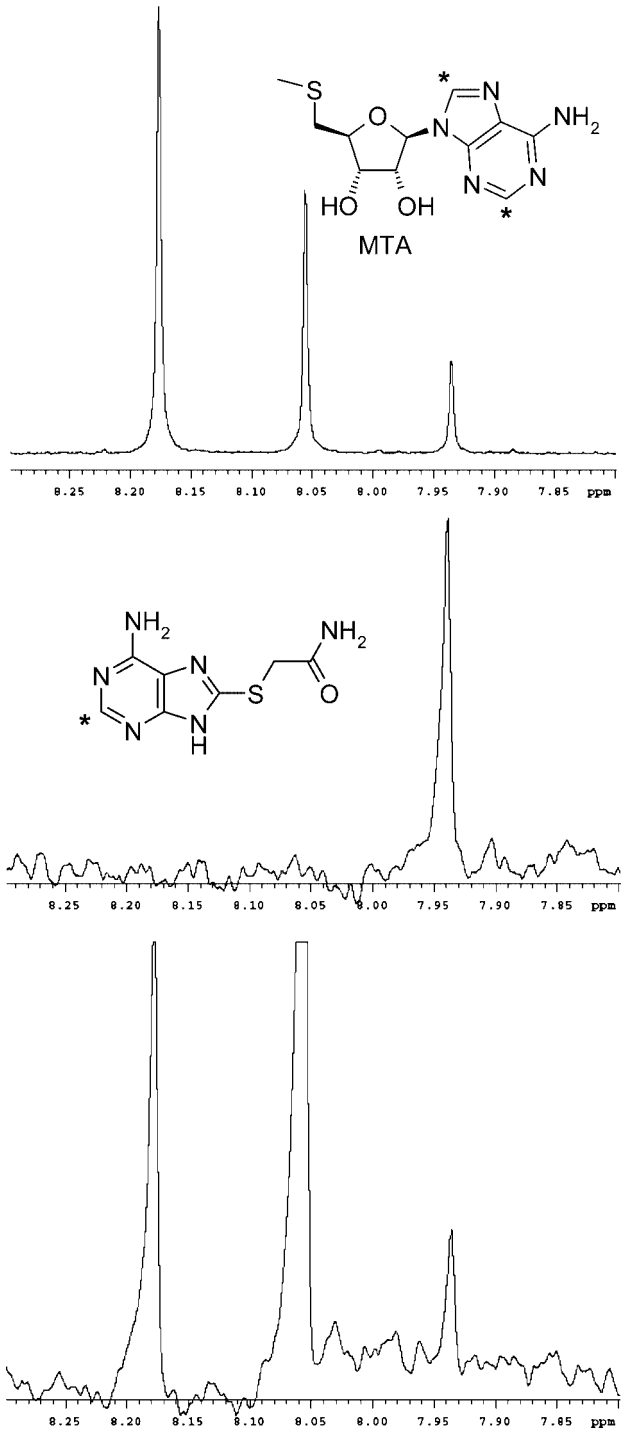

Figure 5. Aromatic regions of the conventional ^{1}H 1D NMR spectrum of MTA and **1** (top), STD NMR spectra with the same vertical scale of **1** and *Pf* SpdSyn (middle), and MTA, **1** and *Pf* SpdSyn (bottom). Structures of MTA and **1** with the displayed proton signals marked with "*" shown for reference. The conclusions from these spectra are (a) that **1** and MTA are soluble in buffer, (b) that **1** clearly binds to *Pf* SpdSyn, and (c) that **1** is partially competed out by a 2.5-fold molar excess of MTA.

The predicted binding poses of **1** and **4** are shown in Figure 7, and the predicted poses of all 8 active site binders are available as PDB files as part of the Supporting Information.

Discussion

The main finding of the present study is the identification of seven novel *Pf* SpdSyn active-site binders. Also, it demonstrates the power of combining 3D pharmacophore filtering with docking and scoring, in this case implemented through a novel combination of two existing virtual screening softwares, Phase[38] and Glide.[39] Additionally, the use of NMR binding experiments to experimentally test binding of compounds from virtual screening is demonstrated.

Table 2. NMR Relaxation Filter Results

compound	relaxation filter	relaxation filter competititon[a]
1	binds	competes
4	binds	binds strongly
5	binds weakly	partial or no competition
10	binds	partial competition
11	binds	no competition
14	binds	partial competition
17	binds	partial competition
25	binds	may bind slightly stronger
26	binds	competes

[a] Competition for binding with 63-fold molar excess of MTA over compound.

The aim of this study was to identify compounds binding reversibly in the active site of *Pf* SpdSyn. The next step on the path to find compounds useful to treat malaria through inhibition of SpdSyn is to explore the structure−activity relationship around these compounds, preferably through iterative structure-based design, which could be facilitated by the high solubility, as judged by NMR signal intensities, and the small size of the novel binders. The predicted pose of compound **1** (see Figure 7) suggests that variation and expansion of the ethylamide moiety could be beneficial, something which could be accomplished, e.g., by alkylating the commercially available building block 6-amino-9*H*-purine-8-thiol with various alkyl halides. Similarly, the predicted pose of **4** (see Figure 7) indicates that 4- or 5- substitutions on the benzimidazole moiety would be allowed. This could be achieved, together with varying the amine part, by reacting various substituted *o*-nitroanilines with suitable aldehydes containing protected amines.[40]

Two compounds especially warrant further comments. Compound **26**, which was found to be a comparably strong binder, is adenosine. Although adenosine has not previously been reported as an inhibitor of *Pf* SpdSyn, it cannot be regarded as very novel because MTA is a known inhibitor with a known binding mode, and they differ only by a hydroxyl substituted for a thiomethyl. This compound was included in the experimental studies because it was nicely identified by the virtual screening procedure as an active site binder, with a final Glide XP rank of 14 (Table 1). Even though it has not been reported as a binder previously, it could be regarded as a positive control. The starting database of compounds was not seeded with known actives. The ability to identify this probable binder from the large database of 2.6 million structures gave a measure of confidence already before acquiring and testing the final compounds. However, adenosine itself will most probably not serve as a basis of future drug discovery efforts against *Pf* SpdSyn.

Compound **4** showed very interesting results. It was first detected as a binder with modest affinity, but when competed with MTA, the binding was markedly stronger. On the basis of the NMR relaxation filter experiments, the affinity could be at least as high as that of MTA. This kind of cooperative binding in NMR binding experiments has been reported previously.[41] This is also analogous to observations presented by Tamu Dufe et al.[22] When trying to crystallize the complex with the substrate mimic 4MCHA (IC_{50} 1.4 μM),[17] a compound with a remarkably low IC_{50} given its small size, no inhibitor could be observed in

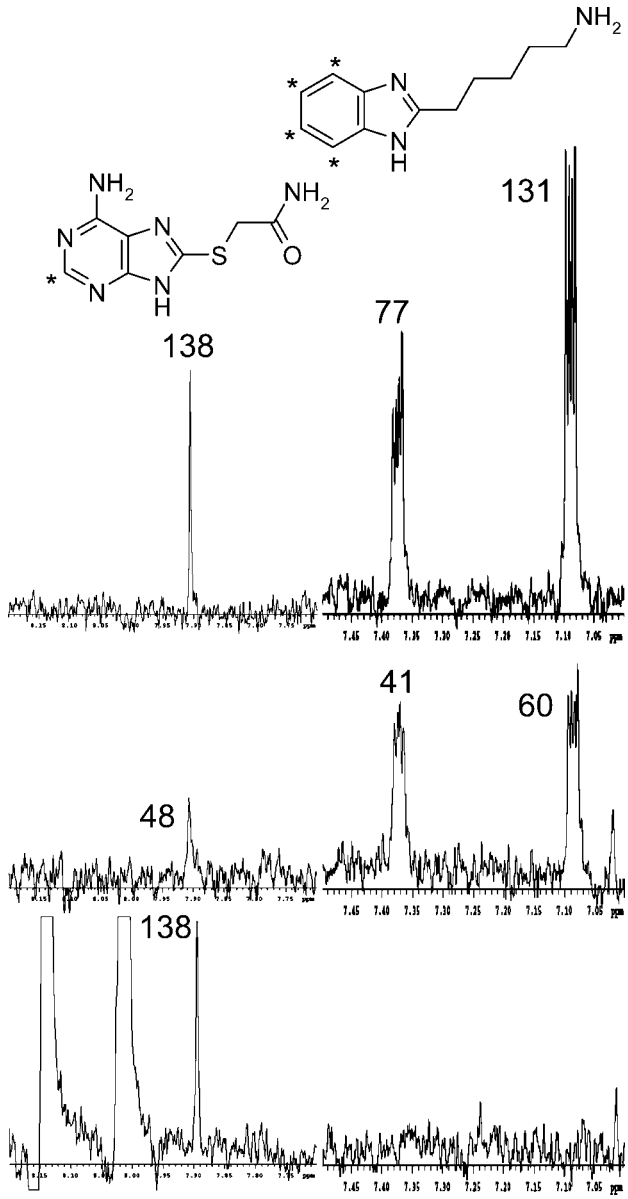

Figure 6. NMR relaxation filter results for **1** (left) and **4** (right). For each compound, three spectra are shown, using the same vertical scaling, and with the same compound concentration in each case. The top spectra are 30 μM compounds in buffer, mid spectra are 30 μM compound and 30 μM protein, and bottom spectra are 30 μM compound, 30 μM protein, and 1880 μM MTA. The structures and the protons corresponding to the displayed NMR signals are indicated with "*" and the heights of each peak is given (arbitrary units). The heights of the peaks are proportional to the concentration of unbound compound.

the active site, even though the protein was incubated with 2.5 mM 4MCHA. However, when the protein was preincubated with dcAdoMet, 4MCHA could be observed in the putrescine binding pocket. The NMR binding results for compound **4** strongly suggest that it binds in the putrescine binding pocket, in a cooperative manner with MTA, and presumably also with dcAdoMet, in the same way as 4MCHA. This is in accordance with the binding pose predicted by Glide XP (see Figure 7). The other compound predicted to bind as an amine substrate mimic, **25**, show the same tendency but to a much smaller degree.

The premises of this study were limited resources for acquiring and testing compounds. Given the relative lack of known inhibitors and structural information on interactions between known inhibitors and the target protein, the task of selecting a few tens of compounds from 2.6 million is rather daunting. To maximize the chances of finding any starting points for generating lead series, the virtual screening procedure outlined in Figure 2 was designed to try to minimize the number of false positives, while not specifically trying to reduce the number of false negatives. Therefore, the first step in this study was a rather severe reduction of the number of candidate compounds, employing 3D pharmacophore filtering of the large database. The idea was that, even if there are many more ways of interacting with the active site and inhibit the protein than the one shown by AdoDATO, considering only compounds predicted to be able to mimic the interactions of this known inhibitor should increase the chance of finding some binders even if testing only a small proportion of the entire database experimentally. On the same note, the Glide SP scores were not used to select compounds, but Glide SP was only used to predict low energy poses of candidate compounds, which are subsequently filtered by their ability to mimic the interactions of AdoDATO. Scoring functions have been shown to correlate with ligand properties such as molecular weight,[42,43] which is a potentially significant source of false positives if selecting compounds from a large diverse set using straightforward docking and scoring and selecting compounds to test based on score alone. Also, the current virtual screening procedure does nothing to decrease the impact of treating the protein as a rigid body, i.e., the problem of not modeling induced fit. Approaches such as using ensembles of protein structures instead of a single rigid structure[44,45] have been suggested, but this is mainly a method to decrease the number of false negatives when used in structure-based virtual screening. Finally, the ultimate selection of compounds to test was made by emphasizing visual inspection of poses according to the hypothesis that these poses are more reliable than the scores. However, it is interesting to note that the three strongest binders identified ranked high in Glide XP score, with rankings of 14, 15, and 111 out of 1866 docked and scored compounds. The worst ranking active site binder had a rank of 301. Both **4** and **1**, relatively strong binders, are small fragment-like molecules with molecular masses of 203 and 224 Da, respectively, that get good scores from Glide XP. In the final set of 1866 compounds docked and scored with Glide XP, high scores biased toward high-molecular-weight compounds did not seem to be a problem.

Biophysical methods such as the NMR binding methods used in this study are especially well suited for testing small sets of predicted binders from structure-based virtual screening. There is no need for assay development, and exactly the predicted event, binding to the active site, is what is observed. If care is taken to identify and deselect unspecific binders, there is no risk of experimental false positives through interference with the assay readout or through inhibiting the protein through other means than reversible binding in the active site such as formation of large aggregates,[46] chemical modification of the protein,[47] or other mechanisms that generally yield false positives in biochemical assays. The methods employed here are also very sensitive, enabling the detection of weak but true binders. One drawback, however, is the lack of information on the potency of the compounds, i.e., the ability of the compounds to modulate the function of the target protein.

Conclusion

Twenty-eight compounds (see Figure 4) were chosen from a database of 2.6 million commercially available screening compounds by a five-step structure-based virtual screening procedure (see Figure 2). Seven of those compounds were found

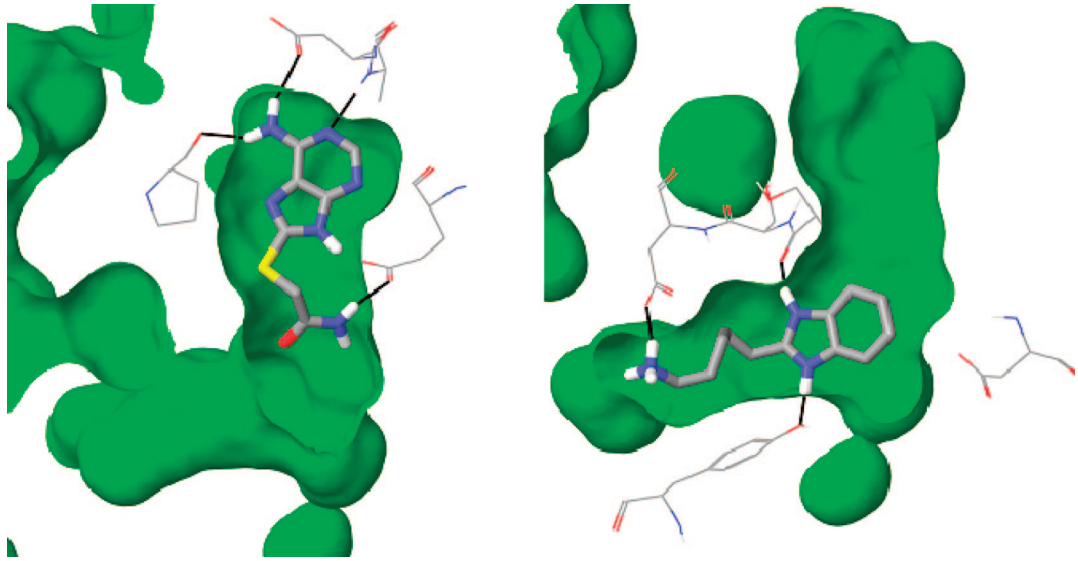

Figure 7. Predicted binding poses of **1** (left) and **4** (right). The molecular surface of the protein is shown in green, hydrogen bonds are shown in black.

to bind reversibly in the active site of *Pf* SpdSyn using STD-NMR and relaxation filter experiments. One additional compound was identified as a weak binder but could not be unambiguously determined to bind in the active site, whereas a ninth binder was found to not bind in the active site.

On the basis of the $T_{1,\rho}$-relaxation filter experiments, assuming fast exchange and approximately equal on-rates, the strongest binders were **4**, but only in the presence of MTA, and **26**. Compound **1** bound almost equally strongly, while **25**, **17**, **14**, and **10** were weaker binders. The relatively small size and high aqueous solubility of these compounds, together with the fact that the 3D structure of the target protein has been solved in complex with a set of small molecules already,[22] could mean that structure determination of *Pf* SpdSyn in complex with these compounds is feasible. This would facilitate the expansion of these hits into lead series, the next step in developing *Pf* SpdSyn inhibitors as pharmaceuticals against malaria.

Experimental Section

Ligand Preparation. The database of chemical structures to screen was constructed from catalogues of commercially available screening compounds from 13 different vendors. Approximately 3 million compounds were compiled into a structurally nonredundant database of 2.8 million structures. These were filtered by molecular weight less than 550 Da and number of rotatable bonds less than or equal to 10 to yield a set of 2.7 million structures. This set was subsequently translated into 3D structures using LigPrep (Schrödinger LLC), generating one stereoisomer, tautomer, and ionization state (the neutral state) for each structure, i.e., one 3D structure per 2D structure in the database. In this process, a number of structures were lost during the minimization stages of LigPrep. The remaining 2.6 million structures were used to construct a Phase database.[38] This entails expanding each structure into conformational ensembles and map pharmacophoric features to each molecule. This Phase database was the starting point for the virtual screen.

During subsequent steps in the virtual screening procedure, compounds were again put through LigPrep but expanded to an ensemble of structures for each compound, representing all relevant stereoisomers, tautomers, and ionization states of each compound. Epik[48] was used to calculate pK_a values for the generation of relevant ionization states.

Target Structures. When this study was initiated, there were two available crystal structures of *Pf* SpdSyn, one complex with MTA (PDB ID 2HTE)[20] and one complex with AdoDATO (PDB ID 2I7C).[22] There are also structures of SpdSyn from *Arabidopsis thaliana*,[49] *Caenorhabditis elegans*,[50] *Homo sapiens*,[51] *Thermotoga maritima*,[52] *Bacillus subtilis, Pyrococcus horikoshii, Pyrococcus furiosis,* and *Thermus thermophilus*. The two *Pf* structures were prepared using the protein preparation workflow implemented in Maestro and Impact (Schrödinger LLC). In short, bond orders and atom types of the ligands were edited manually, waters were removed, and hydrogens added to the protein and ligand structures. The complexes were then minimized until the rmsd between the minimized structure and the starting structure reached 0.3 Å, using OPLS-2005, a version of the OPLS-AA force field.[53]

Docking and Scoring. All docking and scoring calculations were performed using Glide version 4.5.[33,39] The complex with AdoDATO (PDB ID 2I7C) was used as the target structure in the virtual screen because AdoDATO, the ligand of this complex, covers the entire active site and is a more potent inhibitor than MTA. The docking grid size was 8 Å × 12 Å × 14 Å, centered on the center of AdoDATO. This grid encompassed the entire active site pocket. No docking constraints were employed. Glide SP was used in the first docking step of the virtual screening procedure. After pharmacophore filtering, in the final step of the virtual screening procedure, Glide XP docking and scoring were used to sort docked poses and select which compounds to acquire and test during the final visual analysis. In this, the docked structures were grouped by compound ID and sorted by the score of the best scoring structure for each compound.

To validate the use of the Glide SP docking protocol, and the choice of 2I7C as the target structure, a set of known actives,[17,22] MTA, 4MCHA, 5-amino-1-pentene (APE), and AdoDATO, were docked to the target structure and where applicable compared to the experimentally determined binding poses. Note that the experimental pose of APE is not known, and the coordinates of the complex with 4MCHA were not available at the time, but the docked poses of all actives were judged based on the AdoDATO and MTA complexes. As can be seen in Figure 8, the poses predicted by Glide SP using 2I7C as the target structure overlap well with the experimentally determined binding poses of 4MCHA, MTA and AdoDATO.

Pharmacophore Filtering. Phase version 2.0[38] was used to construct 3D pharmacophores and to perform pharmacophore filtering. The 3D pharmacophore models were created using the AdoDATO complex (PDB ID 2I7C) by manually picking pharmacophoric features of the ligand that were hypothesized to be important for the interaction between SpdSyn and AdoDATO. To limit the number of hits, excluded volumes were added manually

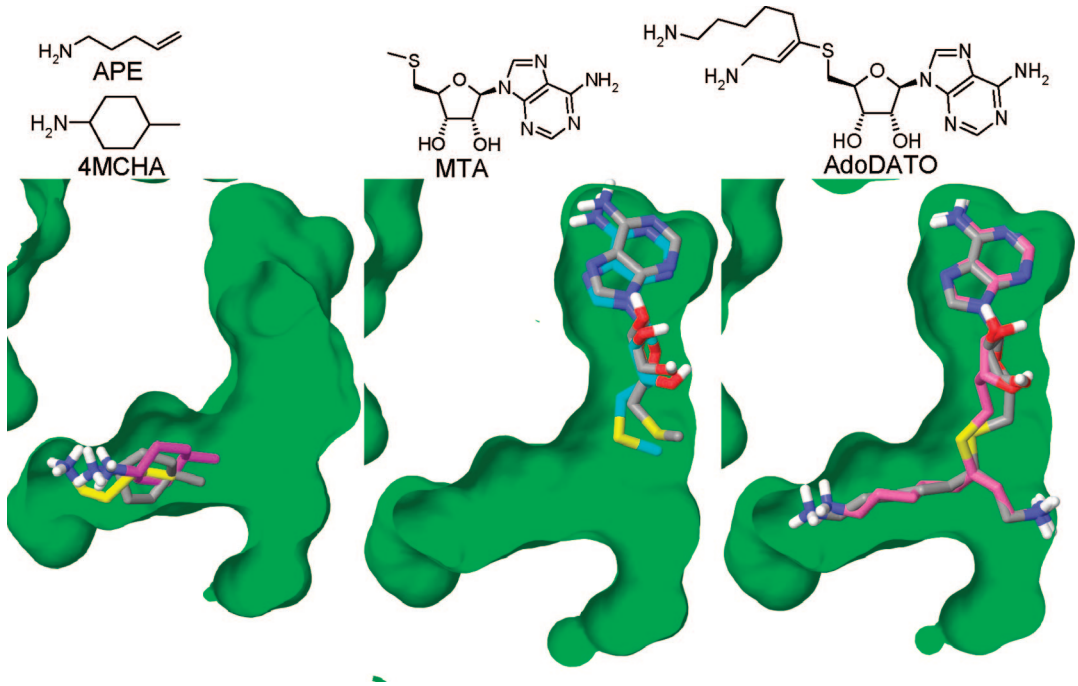

Figure 8. Docked poses of 4MCHA (carbons in magenta) and APE (carbons in yellow), binding in the amino substrate pocket, compared to X-ray pose of 4MCHA (left). MTA (carbons in cyan), binding in the adenosine binding pocket, compared to X-ray pose of MTA (mid) and AdoDATO (carbons in pink), encompassing both subpockets, compared to X-ray pose of AdoDATO (right). The molecular surface of the active site pocket of *Pf* SpdSyn from the AdoDATO complex structure is shown in green.

by picking protein atoms in contact with the ligand. The pharmacophores used are available as Supporting Information. Two separate pharmacophores were created, one intended to describe the interactions between the protein and the adenosine part of AdoDATO and one intended to describe the interactions of the amine substrate mimicking part of AdoDATO, specifically the putrescine binding pocket (see Figure 3). The first pharmacophore contained six features: one hydrogen bond donor and one acceptor corresponding to backbone hydrogen bonds to P203 and A179, one aromatic ring corresponding to the adenine ring, and two hydrogen bond donors and one acceptor corresponding to the hydrogen bond interaction between the hydroxyls of the sugar moiety of AdoDATO and E147 and Q72. The second pharmacophore contained two features: one hydrophobic feature corresponding to the butyl moiety of putrescine and one positively ionizable feature corresponding to one of the terminal primary amine of the substrate, forming an ion−ion interaction with D199. The placement of the hydrophobic feature of the second pharmacophore model was guided using hydrophobic volumes calculated in Maestro.[54] These volumes are isoenergetic surfaces in a potential calculated using a hydrophobic probe.

When the six-point pharmacophore was used to filter the Phase database, at least four features of the pharmacophore were required to match and three of these had to be the two hydrogen bond features and the aromatic ring feature associated with the adenine ring of AdoDATO (see Figure 3). Qualitatively, this can be described as requiring hit compounds to be able to place a group containing an aryl and being able to form the two backbone hydrogen bonds in the adenine-binding subpocket of the active site at the same time as forming at least one of the three hydrogen bond interactions that are formed between the sugar-moiety hydroxyls of AdoDATO and the protein while not violating any of the excluded volumes.

The two-point pharmacophore was applied by requiring both features to match while not violating any excluded volumes.

The distance tolerance was set to its default value of ± 2.0 Å in all pharmacophore searches. Note that the pharmacophore matching score of Phase was not used in the virtual screening procedure. The pharmacophores were applied as binary filters, selecting all matching compounds as hits.

NMR Binding Experiments. All compounds were dissolved and kept as stock solutions in deuterated DMSO at 50 mM. The buffer used in all NMR experiments was 25 mM deuterated Tris and 150 mM NaCl in D_2O, pH 7.6. All NMR experiments were performed at 17 °C. For each sample, a conventional ^{1}H 1D spectrum was collected in addition to the binding experiment. In all conventional ^{1}H 1D spectra, the protein methyl signals showed the resonance dispersion characteristics of a folded protein. MTA was used as a positive control in all batches of binding experiments. The NMR experiments were performed on a Varian Unity Inova 600 MHz NMR spectrometer equipped with a cryogenically cooled probe and a flow cell insert. The samples were loaded into a 96-well plate placed on a Peltier cooling device in order to keep samples waiting to be measured at 6 °C.

The compounds were tested for binding to *Pf* SpdSyn using saturation transfer difference (STD) NMR.[34] Protein saturation was achieved by applying a train of 50 ms Gaussian frequency selective pulses at 0.6 ppm for 2.3 s. The protein and compound concentrations were 10 and 200 μM, respectively, and the DMSO concentration was 0.4%. Identified binders were tested for competition with the known active-site binder MTA, again using STD. The protein, compound, and MTA concentrations were 10, 200, and 500 μM, respectively, and the DMSO concentration was 1.4%.

To confirm the STD results, $T_{1,\rho}$-relaxation filter experiments with a spinlock time of 400 ms were used.[35] All compound stock solutions were diluted to 10 mM in DMSO-d_6, and MTA was additionally prepared as a 2 mM stock solution in buffer. Binding experiments were performed using 30 μM compound and 30 μM protein, DMSO concentration 0.3%. Competition with MTA was performed using the same compound, protein, and DMSO concentrations, adding 1880 μM MTA.

Protein Production. The protein was expressed in *Escherichia coli* and purified as has been described previously,[22,55] with the difference that the N-terminal His-tag was not cleaved off and that the composition of the final buffer was 20 mM HEPES, 300 mM NaCl, 10% glycerol, and 0.5 mM TCEP, pH 7.5. The final protein concentration was estimated to 18 mg/mL, or 532 μM, using A280. The mass of the purified protein (theoretical value 34420 Da) was confirmed using MALDI-MS, giving an experimental value of 34422 Da.

Materials. The plasmid containing the protein construct[55] was received from the Structural Genomics Consortium in Toronto, Canada. MTA was acquired from Sigma-Aldrich (product number D5011). Compounds were acquired from the following sources; **1**(BAS00161987, Asinex), **2** (BAS00185645, Asinex), **3** (BAS01127799, Asinex), **4** (BAS03107294, Asinex), **5** (BAS06347363, Asinex), **6** (BAS09667195, Asinex), **7** (BAS12711444, Asinex), **8** (T0506-2156, Enamine), **9** (T0507-6684, Enamine), **10** (T5229124, Enamine), **11** (T5311846, Enamine), **12** (T5660363, Enamine), **13** (T5712393, Enamine), **14** (T5718184, Enamine), **15** (T5731048, Enamine), **16** (F1284-0724, Life Chemicals), **17** (F3095-3963, Life Chemicals), **18** (STK207415, Vitas-M Laboratories), **19** (G339-0030, Chemdiv), **20** (STK207339, Vitas-M Laboratories), **21** (STK211732, Vitas-M Laboratories), **22** (STK245245, Vitas-M Laboratories), **23** (2T-0822, Keyorganics), **24** (SCR01020, Maybridge), **25** (AQ-387/423026, SPECS), **26** (100036965, ASDI Biosciences), **27** (STOCK4S-2857, Interbioscreen), **28** (7599-1019, Chemdiv).

Acknowledgment. We thank SGC Toronto for supplying the plasmid to produce the protein, Dr. Susanne Gräslund and co-workers for assistance in expressing and purifying the protein, Dr. Natalia Markova and Carina Norström for protein and compound characterization, Dr. Toshiaki Nishida for assistance with NMR experiments, and Dr. Jan Vågberg for organic chemistry advice. We thank the Foundation for Strategic Research (SSF) for financial support.

Supporting Information Available: NMR relaxation filter spectra and results for nine compounds found to bind to *Pf* SpdSyn using STD-NMR experiments, PDB files with the predicted binding poses of the eight active site binders and coordinates of the pharmacophoric features in the two Phase pharmacophores used in the virtual screen. This material is available free of charge via the Internet at http://pubs.acs.org.

References

(1) World Malaria Report 2005; World Health Organization: Geneva, 2005; http://www.rbm.who.int/wmr2005/.
(2) Heby, O.; Roberts, S. C.; Ullman, B. Polyamine biosynthetic enzymes as drug targets in parasitic protozoa. *Biochem. Soc. Trans.* **2003**, *31*, 415–419.
(3) Bitonti, A. J.; McCann, P. P.; Sjoerdsma, A. *Plasmodium falciparum* and *Plasmodium berghei*: effects of ornithine decarboxylase inhibitors on erythrocytic schizogony. *Exp. Parasitol.* **1987**, *64*, 237–243.
(4) Wright, P. S.; Byers, T. L.; Cross-Doersen, D. E.; McCann, P. P.; Bitonti, A. J. Irreversible inhibition of *S*-adenosylmethionine decarboxylase in *Plasmodium falciparum*-infected erythrocytes: growth inhibition in vitro. *Biochem. Pharmacol.* **1991**, *41*, 1713–1718.
(5) Kaiser, A.; Gottwald, A.; Wiersch, C.; Lindenthal, B.; Maier, W.; Seitz, H. M. Effect of drugs inhibiting spermidine biosynthesis and metabolism on the in vitro development of *Plasmodium falciparum*. *Parasitol. Res.* **2001**, *87*, 963–972.
(6) Muller, S.; Coombs, G. H.; Walter, R. D. Targeting polyamines of parasitic protozoa in chemotherapy. *Trends Parasitol.* **2001**, *17*, 242–249.
(7) Kaiser, A.; Gottwald, A.; Maier, W.; Seitz, H. M. Targeting enzymes involved in spermidine metabolism of parasitic protozoa: a possible new strategy for antiparasitic treatment. *Parasitol. Res.* **2003**, *91*, 508–516.
(8) Moritz, E.; Seidensticker, S.; Gottwald, A.; Maier, W.; Hoerauf, A.; Njuguna, J. T.; Kaiser, A. The efficacy of inhibitors involved in spermidine metabolism in *Plasmodium falciparum*, *Anopheles stephensi*, and *Trypanosoma evansi*. *Parasitol. Res.* **2004**, *94*, 37–48.
(9) Das Gupta, R.; Krause-Ihle, T.; Bergmann, B.; Muller, I. B.; Khomutov, A. R.; Muller, S.; Walter, R. D.; Luersen, K. 3-Aminooxy-1-aminopropane and derivatives have an antiproliferative effect on cultured *Plasmodium falciparum* by decreasing intracellular polyamine concentrations. *Antimicrob. Agents Chemother.* **2005**, *49*, 2857–2864.
(10) Tabor, C. W.; Tabor, H. Polyamines. *Annu. Rev. Biochem.* **1984**, *53*, 749–790.
(11) Marton, L. J.; Pegg, A. E. Polyamines as targets for therapeutic intervention. *Annu. Rev. Pharmacol. Toxicol.* **1995**, *35*, 55–91.
(12) Pegg, A. E.; Poulin, R.; Coward, J. K. Use of aminopropyltransferase inhibitors and of non-metabolizable analogs to study polyamine regulation and function. *Int. J. Biochem. Cell Biol.* **1995**, *27*, 425–442.
(13) Hamasaki-Katagiri, N.; Tabor, C. W.; Tabor, H. Spermidine biosynthesis in *Saccharomyces cerevisae*: polyamine requirement of a null mutant of the SPE3 gene (spermidine synthase). *Gene* **1997**, *187*, 35–43.
(14) Guo, K.; Chang, W. T.; Newell, P. C. Isolation of spermidine synthase gene (spsA) of *Dictyostelium discoideum*. *Biochim. Biophys. Acta* **1999**, *1449*, 211–216.
(15) Roberts, S. C.; Jiang, Y.; Jardim, A.; Carter, N. S.; Heby, O.; Ullman, B. Genetic analysis of spermidine synthase from *Leishmania donovani*. *Mol. Biochem. Parasitol.* **2001**, *115*, 217–226.
(16) Park, M. H.; Lee, Y. B.; Joe, Y. A. Hypusine is essential for eukaryotic cell proliferation. *Biol. Signals* **1997**, *6*, 115–123.
(17) Haider, N.; Eschbach, M. L.; Dias Sde, S.; Gilberger, T. W.; Walter, R. D.; Luersen, K. The spermidine synthase of the malaria parasite *Plasmodium falciparum*: molecular and biochemical characterisation of the polyamine synthesis enzyme. *Mol. Biochem. Parasitol.* **2005**, *142*, 224–236.
(18) Metcalf, B. W.; Bey, P.; Danzin, C.; Jung, M. J.; Casara, P.; Vevert, J. P. Catalytic irreversible inhibition of mammalian ornithine decarboxylase (E.C.4.1.1.17) by substrate and product analogs. *J. Am. Chem. Soc.* **1978**, *100*, 2551–2553.
(19) Wang, C. C. Molecular mechanisms and therapeutic approaches to the treatment of African trypanosomiasis. *Annu. Rev. Pharmacol. Toxicol.* **1995**, *35*, 93–127.
(20) Vedadi, M.; Lew, J.; Artz, J.; Amani, M.; Zhao, Y.; Dong, A.; Wasney, G. A.; Gao, M.; Hills, T.; Brokx, S.; Qiu, W.; Sharma, S.; Diassiti, A.; Alam, Z.; Melone, M.; Mulichak, A.; Wernimont, A.; Bray, J.; Loppnau, P.; Plotnikova, O.; Newberry, K.; Sundararajan, E.; Houston, S.; Walker, J.; Tempel, W.; Bochkarev, A.; Kozieradzki, I.; Edwards, A.; Arrowsmith, C.; Roos, D.; Kain, K.; Hui, R. Genome-scale protein expression and structural biology of *Plasmodium falciparum* and related Apicomplexan organisms. *Mol. Biochem. Parasitol.* **2007**, *151*, 100–110.
(21) Coward, J. K.; Pegg, A. E. Specific multisubstrate adduct inhibitors of aminopropyltransferases and their effect on polyamine biosynthesis in cultured cells. *Adv. Enzyme Regul.* **1987**, *26*, 107–113.
(22) Dufe, V. T.; Qiu, W.; Muller, I. B.; Hui, R.; Walter, R. D.; Al-Karadaghi, S. Crystal structure of *Plasmodium falciparum* spermidine synthase in complex with the substrate decarboxylated *S*-adenosylmethionine and the potent inhibitors 4MCHA and AdoDATO. *J. Mol. Biol.* **2007**, *373*, 167–177.
(23) Knox, A. J.; Meegan, M. J.; Sobolev, V.; Frost, D.; Zisterer, D. M.; Williams, D. C.; Lloyd, D. G. Target specific virtual screening: optimization of an estrogen receptor screening platform. *J. Med. Chem.* **2007**, *50*, 5301–5310.
(24) Park, H.; Hwang, K. Y.; Oh, K. H.; Kim, Y. H.; Lee, J. Y.; Kim, K. Discovery of novel alpha-glucosidase inhibitors based on the virtual screening with the homology-modeled protein structure. *Bioorg. Med. Chem.* **2007**, *16*, 284–292.
(25) Bowman, A. L.; Nikolovska-Coleska, Z.; Zhong, H.; Wang, S.; Carlson, H. A. Small molecule inhibitors of the MDM2-p53 interaction discovered by ensemble-based receptor models. *J. Am. Chem. Soc.* **2007**, *129*, 12809–12814.
(26) Luzhkov, V. B.; Selisko, B.; Nordqvist, A.; Peyrane, F.; Decroly, E.; Alvarez, K.; Karlen, A.; Canard, B.; Åqvist, J. Virtual screening and bioassay study of novel inhibitors for dengue virus mRNA cap (nucleoside-2′O)-methyltransferase. *Bioorg. Med. Chem.* **2007**, *15*, 7795–7802.
(27) Park, H.; Kim, Y. J.; Hahn, J. S. A novel class of Hsp90 inhibitors isolated by structure-based virtual screening. *Bioorg. Med. Chem. Lett.* **2007**, *17*, 6345–6349.
(28) Hirayama, K.; Aoki, S.; Nishikawa, K.; Matsumoto, T.; Wada, K. Identification of novel chemical inhibitors for ubiquitin C-terminal hydrolase-L3 by virtual screening. *Bioorg. Med. Chem.* **2007**, *15*, 6810–6818.
(29) Mugnaini, C.; Rajamaki, S.; Tintori, C.; Corelli, F.; Massa, S.; Witvrouw, M.; Debyser, Z.; Veljkovic, V.; Botta, M. Toward novel HIV-1 integrase binding inhibitors: molecular modeling, synthesis, and biological studies. *Bioorg. Med. Chem. Lett.* **2007**, *17*, 5370–5373.
(30) Perola, E. Minimizing false positives in kinase virtual screens. *Proteins* **2006**, *64*, 422–435.
(31) Brenk, R.; Naerum, L.; Gradler, U.; Gerber, H. D.; Garcia, G. A.; Reuter, K.; Stubbs, M. T.; Klebe, G. Virtual screening for submicromolar leads of tRNA-guanine transglycosylase based on a new unexpected binding mode detected by crystal structure analysis. *J. Med. Chem.* **2003**, *46*, 1133–1143.
(32) Muthas, D.; Sabnis, Y. A.; Lundborg, M.; Karlen, A. Is it possible to increase hit rates in structure based virtual screening by pharmacophore filtering? An investigation of the advantages and pitfalls of post-filtering. *J. Mol. Graph. Modell.* **2007**, dx.doi.org/10.1016/j.jmgm.2007.11.005.

(33) Friesner, R. A.; Murphy, R. B.; Repasky, M. P.; Frye, L. L.; Greenwood, J. R.; Halgren, T. A.; Sanschagrin, P. C.; Mainz, D. T. Extra precision glide: docking and scoring incorporating a model of hydrophobic enclosure for protein−ligand complexes. *J. Med. Chem.* **2006**, *49*, 6177–6196.

(34) Mayer, M.; Meyer, B. Characterization of Ligand Binding by Saturation Transfer Difference NMR Spectroscopy. *Angew. Chem., Int. Ed. Engl.* **1999**, *38*, 1784–1788.

(35) Hajduk, P. J.; Olejniczak, E. T.; Fesik, S. W. One-Dimensional Relaxation- and Diffusion-Edited NMR Methods for Screening Compounds That Bind to Macromolecules. *J. Am. Chem. Soc.* **1997**, *119*, 12257–12261.

(36) van Dongen, M.; Weigelt, J.; Uppenberg, J.; Schultz, J.; Wikstrom, M. Structure-based screening and design in drug discovery. *Drug Discovery Today* **2002**, *7*, 471–478.

(37) van Dongen, M. J.; Uppenberg, J.; Svensson, S.; Lundback, T.; Akerud, T.; Wikstrom, M.; Schultz, J. Structure-based screening as applied to human FABP4: a highly efficient alternative to HTS for hit generation. *J. Am. Chem. Soc.* **2002**, *124*, 11874–11880.

(38) Dixon, S. L.; Smondyrev, A. M.; Knoll, E. H.; Rao, S. N.; Shaw, D. E.; Friesner, R. A. PHASE: a new engine for pharmacophore perception, 3D QSAR model development, and 3D database screening: 1. Methodology and preliminary results. *J. Comput.-Aided Mol. Des.* **2006**, *20*, 647–671.

(39) Friesner, R. A.; Banks, J. L.; Murphy, R. B.; Halgren, T. A.; Klicic, J. J.; Mainz, D. T.; Repasky, M. P.; Knoll, E. H.; Shelley, M.; Perry, J. K.; Shaw, D. E.; Francis, P.; Shenkin, P. S. Glide: a new approach for rapid, accurate docking and scoring. 1. Method and assessment of docking accuracy. *J. Med. Chem.* **2004**, *47*, 1739–1749.

(40) Yang, D.; Fokas, D.; Li, J.; Yu, L.; Baldino, C. A Versatile Method for the Synthesis of Benzimidazoles from *o*-Nitroanilines and Aldehydes in One Step via a Reductive Cyclization. *Synthesis* **2005**, 47–56.

(41) Huth, J. R.; Park, C.; Petros, A. M.; Kunzer, A. R.; Wendt, M. D.; Wang, X.; Lynch, C. L.; Mack, J. C.; Swift, K. M.; Judge, R. A.; Chen, J.; Richardson, P. L.; Jin, S.; Tahir, S. K.; Matayoshi, E. D.; Dorwin, S. A.; Ladror, U. S.; Severin, J. M.; Walter, K. A.; Bartley, D. M.; Fesik, S. W.; Elmore, S. W.; Hajduk, P. J. Discovery and design of novel HSP90 inhibitors using multiple fragment-based design strategies. *Chem. Biol. Drug. Des.* **2007**, *70*, 1–12.

(42) Jacobsson, M.; Karlen, A. Ligand bias of scoring functions in structure-based virtual screening. *J. Chem. Inf. Model.* **2006**, *46*, 1334–1343.

(43) Pan, Y.; Huang, N.; Cho, S.; MacKerell, A. D. Consideration of molecular weight during compound selection in virtual target-based database screening. *J. Chem. Inf. Comput. Sci.* **2003**, *43*, 267–272.

(44) Nabuurs, S. B.; Wagener, M.; de Vlieg, J. A flexible approach to induced fit docking. *J. Med. Chem.* **2007**, *50*, 6507–6518.

(45) Sherman, W.; Day, T.; Jacobson, M. P.; Friesner, R. A.; Farid, R. Novel procedure for modeling ligand/receptor induced fit effects. *J. Med. Chem.* **2006**, *49*, 534–553.

(46) McGovern, S. L.; Caselli, E.; Grigorieff, N.; Shoichet, B. K. A common mechanism underlying promiscuous inhibitors from virtual and high-throughput screening. *J. Med. Chem.* **2002**, *45*, 1712–1722.

(47) Tjernberg, A.; Hallen, D.; Schultz, J.; James, S.; Benkestock, K.; Bystrom, S.; Weigelt, J. Mechanism of action of pyridazine analogues on protein tyrosine phosphatase 1B (PTP1B). *Bioorg. Med. Chem. Lett.* **2004**, *14*, 891–895.

(48) Shelley, J. C.; Cholleti, A.; Frye, L. L.; Greenwood, J. R.; Timlin, M. R.; Uchimaya, M. Epik: a software program for pK_a prediction and protonation state generation for drug-like molecules. *J. Comput.-Aided Mol. Des.* **2007**, *21*, 681–691.

(49) Levin, E. J.; Kondrashov, D. A.; Wesenberg, G. E.; Phillips, G. N. Ensemble refinement of protein crystal structures: validation and application. *Structure* **2007**, *15*, 1040–1052.

(50) Dufe, V. T.; Luersen, K.; Eschbach, M. L.; Haider, N.; Karlberg, T.; Walter, R. D.; Al-Karadaghi, S. Cloning, expression, characterisation and three-dimensional structure determination of *Caenorhabditis elegans* spermidine synthase. *FEBS Lett.* **2005**, *579*, 6037–6043.

(51) Wu, H.; Min, J.; Ikeguchi, Y.; Zeng, H.; Dong, A.; Loppnau, P.; Pegg, A. E.; Plotnikov, A. N. Structure and mechanism of spermidine synthases. *Biochemistry* **2007**, *46*, 8331–8339.

(52) Korolev, S.; Ikeguchi, Y.; Skarina, T.; Beasley, S.; Arrowsmith, C.; Edwards, A.; Joachimiak, A.; Pegg, A. E.; Savchenko, A. The crystal structure of spermidine synthase with a multisubstrate adduct inhibitor. *Nat. Struct. Biol.* **2002**, *9*, 27–31.

(53) Jorgensen, W. L.; Maxwell, D. S.; Tirado-Rives, J. Development and Testing of the OPLS All-Atom Force Field on Conformational Energetics and Properties of Organic Liquids. *J. Am. Chem. Soc.* **1996**, *118*, 11225–11236.

(54) *Maestro 8.0 User Manual*, Revision A; Schrödinger Press: New York, 2007; p 274.

(55) Structural Genomics Consortium Materials and Methods, PDB ID 2HTE; Structural Genomics Consortium: Toronto, 2006; http://www.sgc.utoronto.ca/SGC-WebPages/StructureDescription/MM.php?pdb=2HTE.

JM7016144